Journal of Structural Geology, Vol. 1, No. 1, pp. 19 to 30.
Pergamon Press Ltd. 1979. Printed in Great Britain

The development of asymmetrical folds in a cross-laminated siltstone

P. F. WILLIAMS
Geologisch en Mineralogisch Instituut der R.U., Garenmarkt 1B, Leiden, Holland

(*Received* 25 *September* 1978; *accepted in revised form* 5 *December* 1978)

Abstract—A group of folds in alternating pelites and cross-laminated siltstones is described. An interpretation of the finite strain state, in the competent silt layers, is proposed on the basis of an analysis of the angle between cross-lamination and the principal surface of accumulation. Strain magnitudes are greatest in the fold hinge where domains of layer parallel shortening and layer parallel extension are separated by a neutral surface. Strain magnitudes in the fold limbs are small and are largely related to the development of the asymmetry of the folds. In the incompetent pelitic layers, strain in the fold limbs has a large, layer parallel shear component. Deformation in the pelites is accompanied by, and presumably partially achieved by, migration of quartz from areas where there is a tendency for volume to decrease, to areas where it is tending to increase. This process involves local increases in volume of more than 50%.

A kinematic model is proposed for development of the folds. It involves early development of small symmetrical folds followed by their modification to asymmetrical, parasitic structures on the limbs of later folds. In the late stages of folding, continued shortening perpendicular to the axial surface orientation is achieved by development of a conjugate crenulation cleavage.

INTRODUCTION

IT IS generally difficult to extract information from natural folds concerning the patterns of strain and deformational histories associated with them. The folds described here allow an unusual amount of such information to be obtained because they fold continuous, cross-laminated beds. Quantitative strain analysis of the cross-lamination is not possible (see Hobbs & Talbot 1966). Nevertheless this marker provides much information about variation in strain around the fold, and thus makes an interpretation of the deformation history possible.

The folds are from Palaeozoic turbidites from the South Coast region of New South Wales and are from the cliff just south of Bermagui Head. These rocks have been multiply deformed and metamorphosed under greenschist facies conditions (Williams 1971). The folds involve a series of alternating pelitic beds and micro-cross-laminated, silty beds.

A specimen was selected for detailed analysis. It was cut to produce a flat surface including the maximum number of folds, and because of this the surface is not parallel to the fold profile. The relationship between the section and the folds is shown in Fig. 1.

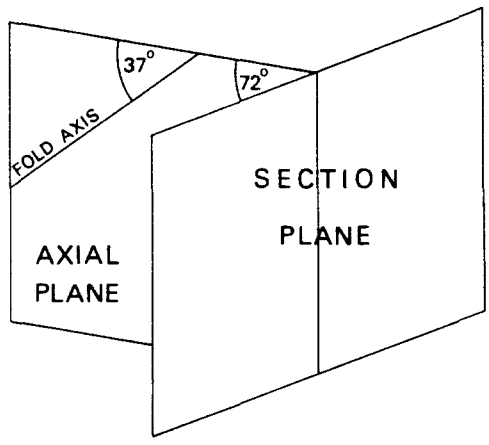

Fig. 1. Geometrical relationship between the section plane (see Fig. 2) and folds.

DESCRIPTION OF FOLDS AND CLEAVAGE

The folds have angular hinges, long, fairly straight limbs (Fig. 2), and are cylindrical on the scale of a hand specimen. There is thickening of the hinges in both siltstone and pelite beds but the thickening is greatest in the latter, so that the siltstone was apparently more competent than the pelite. Taken in pairs the siltstone and pelite layers are approximately similar in form (Fig. 2). The siltstone layers are markedly lenticular (Fig. 2) and part of this variation in thickness is believed to be a primary sedimentary feature since there is no distortion of foreset-topset relationships, and since such primary lenticular forms are common in cross-laminated beds.

There is a well developed differentiated crenulation cleavage parallel to the axial plane in the pelitic beds but no axial plane foliation in the cross-laminated beds. Two sets of later crenulation cleavages overprinting both folds and axial plane foliation are interpreted as members of a conjugate pair. The bisector of the acute dihedral angle of the cleavage pair is inclined to the perpendicular to the axial surface of the small folds by approximately 10°. These small folds, however, are parasitic on larger symmetrical structures and the conjugate cleavage surfaces are symmetrical with respect to the axial surface of these larger structures.

CROSS-LAMINATION

Cross-lamination is readily visible to the unaided eye. In the long straight limbs of the small asymmetric folds the foreset beds make an angle (θ) of between 24° and

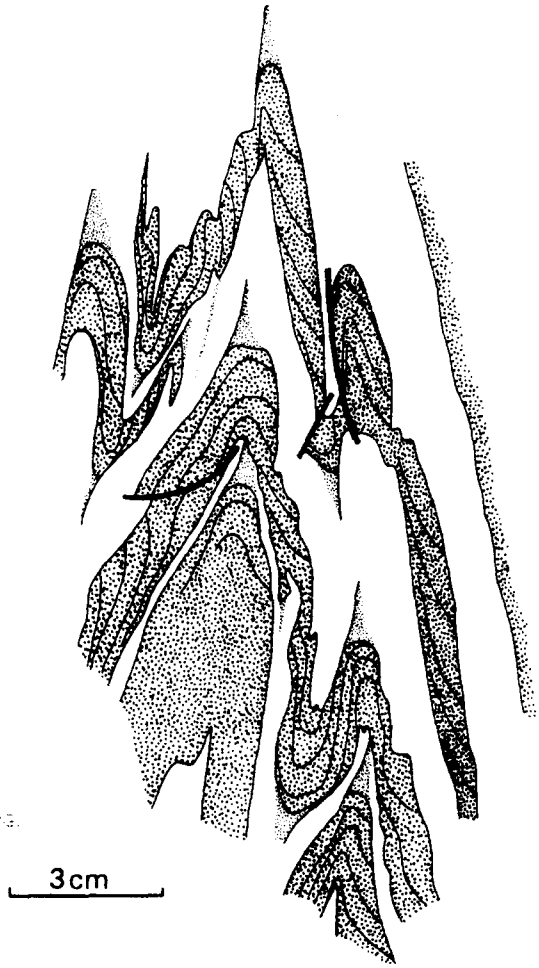

Fig. 2. Folds as seen in the section plane (see Fig. 1). Siltstone layers are stippled and their cross-lamination is shown. Pelitic layers are unornamented, except in areas of quartz concentration where they are faintly stippled. Note that within the pelite, the concentrations mostly have a sharp boundary on one side and not on the other. It is the left hand side for all antiforms and the right hand side for all synforms. Heavy lines indicate small faults.

38° with the topset beds. Sixteen measurements of θ were made on right dipping limbs and seven on left dipping limbs of the specimen illustrated in Fig. 2. These measurements were all made in straight limb areas where there are no rapid changes in θ as there are in the fold closures. In the hinge the angle approaches 0° on the convex side of the fold, and approaches 90° on the concave side of the fold. Accurate measurement is not possible in this area because of the small radius of curvature, and because the surfaces are less sharply defined. The change from the angles measured in the limbs to the larger or smaller angles in the fold hinges occurs in most cases over a very short distance either side of the hinge line (Fig. 2).

The line of intersection of the foreset and topset beds is approximately parallel to the fold axis. Examination of surfaces ground parallel to bedding around two fold closures revealed some variation in the orientation of this line but the largest discrepancy measured between it and the fold axis is less than 5°. Thus a foreset dip measured on the fold profile will deviate from the true dip by less than 1°. However, since the section is not parallel to the profile plane the dip measured on the section is an apparent dip and must be corrected to give the true dip. Corrections were made and the results averaged for right and left dipping limbs. Average dips are 27.6° on right dipping limbs and 40.0° on left dipping limbs. The parallel and perpendicular orientations of the hinge areas remain unchanged.

COMPOSITIONAL VARIATION

Close examination of the pelite reveals a large compositional variation that is of secondary origin. There are domains that are rich in quartz and domains that are rich in layer-silicates. These compositional domains occur in two forms: (a) as a layering defined by alternation of the two types of domain that is statistically parallel to the fold axial surface; (b) quartz-rich domains occur as prismatic bodies in the fold hinges (faintly stippled areas in Fig. 2) elongate parallel to the fold axis. Both types of domain are visible in hand specimen. Under the microscope (Fig. 3) the layering is seen to be related to an axial plane crenulation cleavage. This cleavage, which in the limbs is everywhere synthetic, is differentiated so that the layer-silicate-rich domains alternate with quartz-rich domains, both of which are generally less than 15μm wide. The relative widths of the domains vary, and there are zones in which one type of domain is dominant over the other, thus giving rise to the millimetre scale layering visible in hand specimen and to an even larger scale variation around a fold. Thus on the scale of a fold, mica-rich areas are those in which the mica-rich domains of the crenulation cleavage are broader than the quartz-rich domains. The converse applies to the quartz-rich areas. In the areas richest in layer-silicates the cleavage is a penetrative slaty cleavage, but spatially there is a morphological transition between this cleavage and the differentiated crenulation cleavage. The transition takes the form of a gradual appearance and then widening of the quartz-rich domains and has been discussed in an earlier paper (Williams 1972).

The prismatic quartz-rich domains generally lack a cleavage. Layer-silicates in these areas tend to vary in orientation but where there is a preferred orientation it is parallel to bedding. These domains have an approximately triangular or trapezoidal profile. They occur in fold hinges on the convex side of the competent siltstone beds, and are triangular where they terminate within the pelite. If the pelite is thin, a trapezoidal prism may extend from one siltstone layer to the next. The trapezoid tapers from the convex side of the hinge in one siltstone to the concave side of the hinge in the other. The boundaries of the quartz-rich domains, that lie within the pelite, are generally sharp but one is consistently sharper than the other, and with equal consistency the sharp boundary is on one side for all antiformal closures, and on the opposite side for all synformal closures (Fig. 2).

On the scale of a fold the compositional variation in the pelites is systematic. The prismatic, quartz-rich domains form the core of a larger, layered, quartz-rich

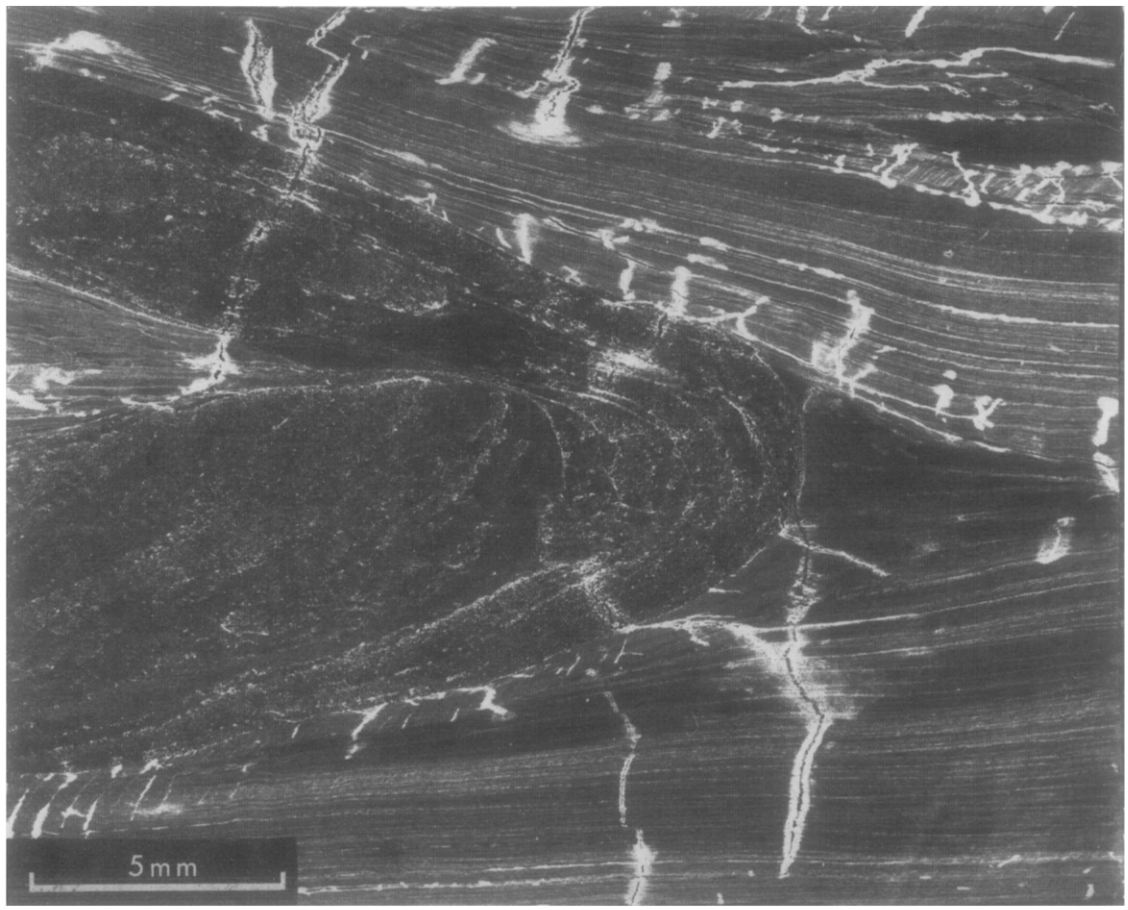

(a)

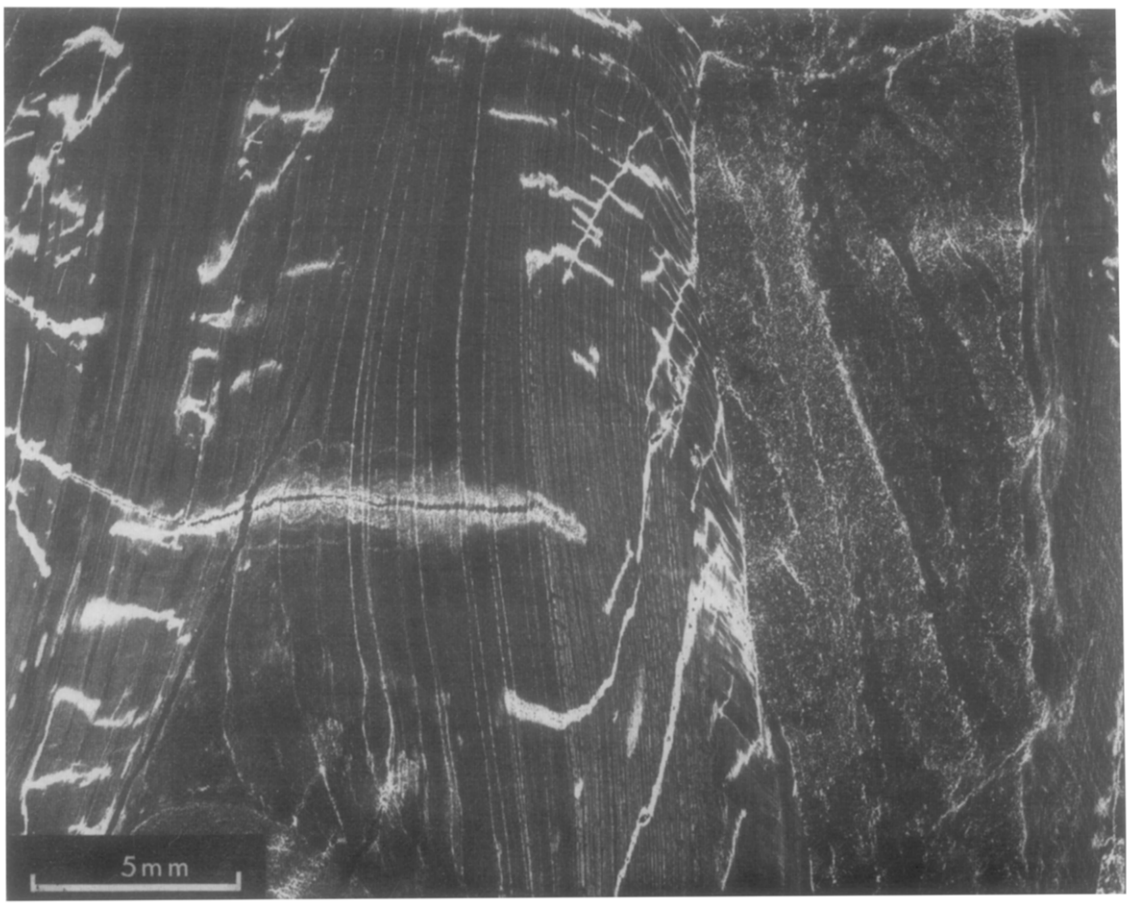

(b)

Fig. 3. Negative photomicrographs of two of the antiforms shown in Fig. 2. The antiform in the cross-laminated layer in (b) is just visible in the bottom left corner. Quartz-rich (dark) triangular areas can be seen on the convex side of the competent layer folds in both (a) and (b). In both antiforms the left hand contact of the domain is sharper than the right hand one. Folded cross-lamination and late stage crenulation cleavage are also visible. The latter is non penetrative and is approximately parallel to the diagonals of the photographs.

area which has approximately the same shape as the core. Mica-rich areas in the pelitic beds are found on fold limbs and on the concave side of hinges in the siltstone beds where the pelite is thick compared to the adjacent siltstones. The magnitude of the variation in composition is well demonstrated in Fig. 3. The layer silicate content of the quartz-rich domain of the fold illustrated in Fig. 3(b) is estimated under the microscope at 40% and that of the layer-silicate-rich domain at 10%. Where this same horizon is involved in the next fold closure and is therefore on the concave side of the competent layer, there is no quartz visible in thin section.

FINITE STRAIN STATE IN CROSS-LAMINATED BEDS

Hobbs & Talbot (1966) have pointed out that it is impossible to make quantitative strain determinations from deformed cross-lamination without making unreasonable assumptions. However, a useful qualitative analysis of the strain is possible if the following reasonable assumptions are made. First it is assumed that the slope of the foreset laminations within a given cross-laminated bed was initially constant. Examination of this structure in planar fold limbs and in undeformed rocks indicates that this is a reasonable assumption. It is also assumed that the strain is plane with no extension parallel to the fold axis. If a uniform extension or shortening has occurred in this direction it will affect the strain magnitudes discussed here, but qualitatively the strain picture will remain essentially the same. Having made these assumptions it follows that:

(1) Since θ tends towards zero on the convex side of fold closures there must be a layer parallel extensional component of strain in that region. Similarly there must be a layer parallel shortening component of strain on the concave side where the angle tends towards 90°. Because in both cases the values of θ are improbable values for the initial dip of the foreset lamination and because there is no evidence of large volume changes, both the shortening and extension are believed to be real. Evidence of volume change is seen elsewhere in these rocks (this paper and Williams 1972).

(2) Since the angle θ is not the same on both fold limbs at least one must have undergone strain. However, the required strain magnitudes may be quite small. For example, assuming an initial value of 30° for θ, plane strain, no volume change, and finite strain axes orthogonal to layering (Fig. 4a), a layer parallel extension of approximately 5% on right dipping limbs and a shortening of approximately 17% on left dipping limbs will produce the observed values. Alternatively, if it is assumed that the observed difference is related to simple shear parallel to the principal surface of accumulation (Fig. 4b), then, with an assumed original value for θ of 30°, a shear of about 0.2 is required on the right dipping limbs and a shear of about 0.57 on the left dipping limbs. The sense of shear is the reverse of that which operates in the flexural slip fold model.

Though not necessary, the finite strain magnitudes may be greater in the fold limbs. The strains quoted above are based on the assumption that the original dip of the foreset beds was 30°. It is unlikely that the dip was initially much greater since the maximum angle of repose for such sediments is close to 30° (see Pettijohn 1957), however, it is certainly possible that the dip was originally much lower. The cross-lamination is asymptotic with the principal surface of accumulation, and the slope therefore varies between a maximum value and zero. Thus the maximum measurable value is a function of the original maximum steepness and the depth to which the original cross-lamination has been eroded (i.e. the steepest part of the foreset bed, as now seen, need

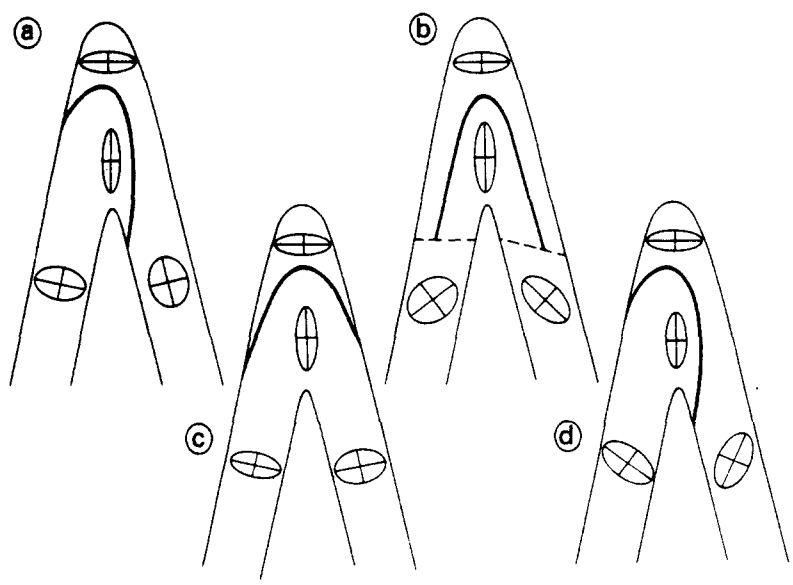

Fig. 4. Possible interpretations of strain for the folds described in this paper. Ellipses are qualitative. Heavy lines are traces of the neutral surfaces and the broken lines separate areas of bedding parallel simple shear (fold limbs), from an area in which there has been bedding parallel extension or shortening. For further discussion see text.

not have been the steepest part of the original ripple form).

If the initial dip was much less than 30° the strain in some areas will be higher than that suggested above. For example, if an initial dip of 10° and plane strain with strain axes orthogonal with bedding is assumed (Fig. 4c), shortenings of about 42 and 54% respectively are required in the two fold limbs to produce the observed angles. In the hinge the shortening will be greater on the concave side of the folded layer, but on the convex side, less extension is required.

The above models assume special relationships between the finite strain ellipsoid and the folded surface, viz. in Figs. 4(a) and (c) the principal axes are orthogonal with the folded surface, and in Fig. 4(b) the circular section is parallel to the folded surface. More general relationships are equally possible. For example in Fig. 4(d) the strain ellipse is oriented so that the strain has a shear component parallel to the folded surface as well as a shortening or extensional component parallel to the same direction. The shear component has the same sense as that of the flexural slip fold model, so that for initially left dipping cross lamination it will tend to reduce the value of θ on left dipping limbs, and increase it on right dipping limbs. This is the opposite of what is observed. However, the effect of the shear component can be reversed by an appropriate layer parallel shortening on left dipping limbs, and by layer parallel extension on right dipping limbs.

The four strain models described above (Fig. 4) are all equally capable of explaining the geometrical relationships observed in the natural folds, so that on purely geometrical grounds it is not possible to choose between them.

STRAIN IN THE PELITIC BEDS

The patterns of strain suggested here for the competent siltstone beds demand large strains in the pelites which must have been constrained to occupy the space between the competent beds. Thus larger shear strains parallel to bedding are to be expected in the fold limbs, and a migration of material from the limbs towards the hinge must also occur (see Ramsay 1974). The migration may occur by flow of a portion of the rock as a whole, but it is also achieved in part by migration of certain components from one area to another.

It has been demonstrated in an earlier paper (Williams 1972) that the layer-silicate-rich domains of the crenulation cleavage develop by migration of quartz out of the layer-silicate-rich domains into either or both microlithons or rocks external to the system. This migration probably takes place in aqueous solution. It was suggested in the earlier paper that the quartz was removed selectively from 'channel ways' that were kept open by deformation. These 'channel ways' thus became the layer-silicate-rich domains. A second possibility is that the layer-silicates behave as strong fibres and induce pressure gradients within the crenulations. Such a mechanism is believed to operate in artificial schists made from salt and mica (Means & Williams 1972) and could apply here. In either case the fold scale migration is believed to occur in reponse to pressure gradients related to stress distributions in the developing fold, and the observations recorded here agree with the stress distributions determined by finite element analysis of viscous fold models (Stephansson 1974).

Whatever the mechanism, the volume changes believed to have occurred in the pelitic layers are consistent with the strains required for them to fill the space between the deforming competent layers. Close to the concave side of a hinge in a competent layer the volume will tend to decrease and this conclusion is consistent with the observed mica-rich zone. Similarly, in the fold limbs a volume decrease is to be expected and again these are mica-rich zones. On the convex side of competent layer fold closures there will be a tendency for volume to increase relative to the other areas. It is not clear that there has been a real increase in this area because if quartz has been introduced, it has not been emplaced as veins but simply as a fine grained matrix. However, if the composition of the prismatic quartz-rich domain is its original composition, the pelites were originally abnormally quartz-rich and the volume of material lost in the development of the folds is substantial. Furthermore the fact that there is a real extension parallel to bedding in this part of the fold suggests that the volume increase in the pelite bed is probably also real; and thus quartz has probably been added.

Stephansson (1974) has shown that where two competent layers are in close proximity the isopachs tend to join one competent layer to the other. This is consistent with the observation that the prismatic quartz-rich domains join two competent layers where they are close together.

POSSIBLE FOLD MODELS FOR THE CROSS-LAMINATED BEDS

From the strain implicit in a given fold model it is possible to predict the geometry of a cross-laminated bed folded in accordance with the model. Ramsay has considered the effects of three fold models on the dihedral angle between foreset laminations and the principal surface of accumulation. The models are flexural slip folding with or without homogeneous flattening (Ramsay 1961, 1967, chapter 9), shear folding with or without homogeneous flattening (Ramsay 1961, 1967, chapter 9), and folding by tangential longitudinal strain (Ramsay 1967, fig. 9.20). The dihedral angles vary from point to point in the various folds and the patterns of variation are diagnostic for each model. Here, these patterns are compared with the natural example.

FLEXURAL SLIP AND SHEAR FOLD MODELS

The pattern observed in the material described here is incompatible with the flexural slip (or flow) and shear fold models. Considering only the configuration of the folded bedding, a homogeneously flattened flexural slip

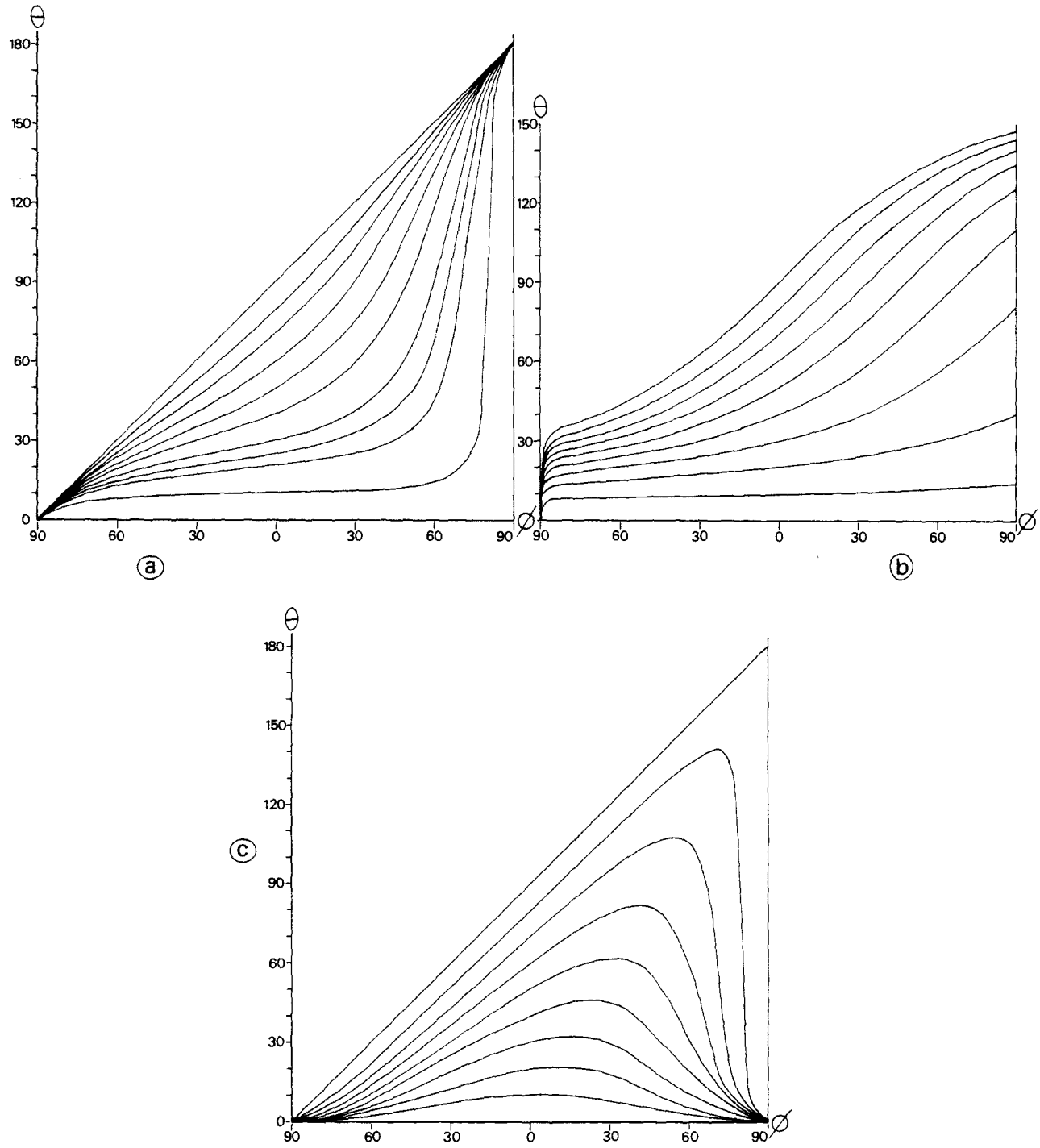

Fig. 5. Graphs of dihedral angles (θ) between foresets and principal accumulation surfaces as a function of the dip (ϕ)of the principal accumulation surface. Values of θ for $\phi = 0$ give the initial (pre-deformation) values of θ for each curve. (a) For kink fold formed by layer parallel progressive simple shear. Angular shear is given by $\psi = \phi$. (b) For flexural slip (flow) fold where fold can be represented by circular arcs and angular shear is therefore given by $\psi = \tan \phi$ rad (see Ramsay 1967, p.393). (c) For shear fold model. Angular shear is given by $\psi = \phi$.

folding is possible, but shear folding with or without flattening is improbable because the folds do not have true similar form. Shear folding, however, cannot be eliminated with certainty on these grounds because the initial bed thickness is believed to have varied although the pattern of variation is unknown. Both models however can be eliminated if the dihedral angles are considered. In this respect there are two features common to both models that do not occur in the real folds.

(a) In both models the strain at various points in the axial plane is identical, and therefore the dihedral angle as seen on the fold profile will be the same at all points along the axial plane trace. In contrast, in the specimen the greatest variation in the magnitude of the dihedral angle occurs along this line.

(b) Both the flexural slip and the shear fold models result in an asymmetry of dihedral angle magnitudes in a traverse across a fold profile. This is demonstrated in

graphs of dihedral angle as a function of principal accumulation surface dip, for two extreme cases of flexural slip folding, and for shear folding (Fig. 5). Flexural slip cannot be represented by a single graph because in such folds strain is a function not only of dip but also of fold shape.

In all cases, if the foresets initially dip left, the dihedral angles on left dipping fold limbs are smaller after deformation than on right dipping limbs. Homogeneous flattening perpendicular to the axial surface does not change this basic pattern as can be seen in Fig. 6 where a fold of similar geometry to the real folds has been analysed in terms of flexural slip folding followed by homogeneous flattening. Figure 6a is traced from one of the natural folds. Using the method first described by Ramsay (1967, pp. 411–415), but in the form expressed by Milnes (1971), log T/log A and log A/log t values for both limbs have been plotted on the graph of Milnes, and of the three sets of measurements made, all give $\Delta\Sigma s$ values between 0.6 and 0.7. Thus if the fold is assumed to have developed by a pure flexural slip (or flow) stage followed by homogeneous flattening, the flattening is about 48%. Figure 6b shows the same fold in its pre-flattening form and it can be seen that there is a variation in limb thickness. If the model were assumed to be applicable the variation could be explained as an original variation in bed thickness. Figures 6(c–e) show the configuration of cross-laminated beds for a fold similar to that shown in (a), for various initial values of θ, assuming flexural flow and 48% later flattening. For ease of construction a constant initial bed thickness has been assumed; this does not make a significant difference to the results. 'Initial value' of θ is used here in the sense of the value at the beginning of flexural flow, and does not include any homogeneous flattening that may have occurred before flexure. It can be seen from Figs. 6(c–e), that, in contrast to the natural material, the initially left dipping foresets have a smaller dihedral angle in the right dipping fold limbs than in those dipping left. Thus flexural flow followed by flattening perpendicular to the axial surface can also be rejected as a possible model.

Another possibility that must be considered is flexural slip followed by a homogeneous flattening that is not orthogonal with the fold axial surface. It is possible that by varying magnitude and orientation, a homogeneous flattening could be found that is capable of producing the observed geometry from a flexural slip fold. This

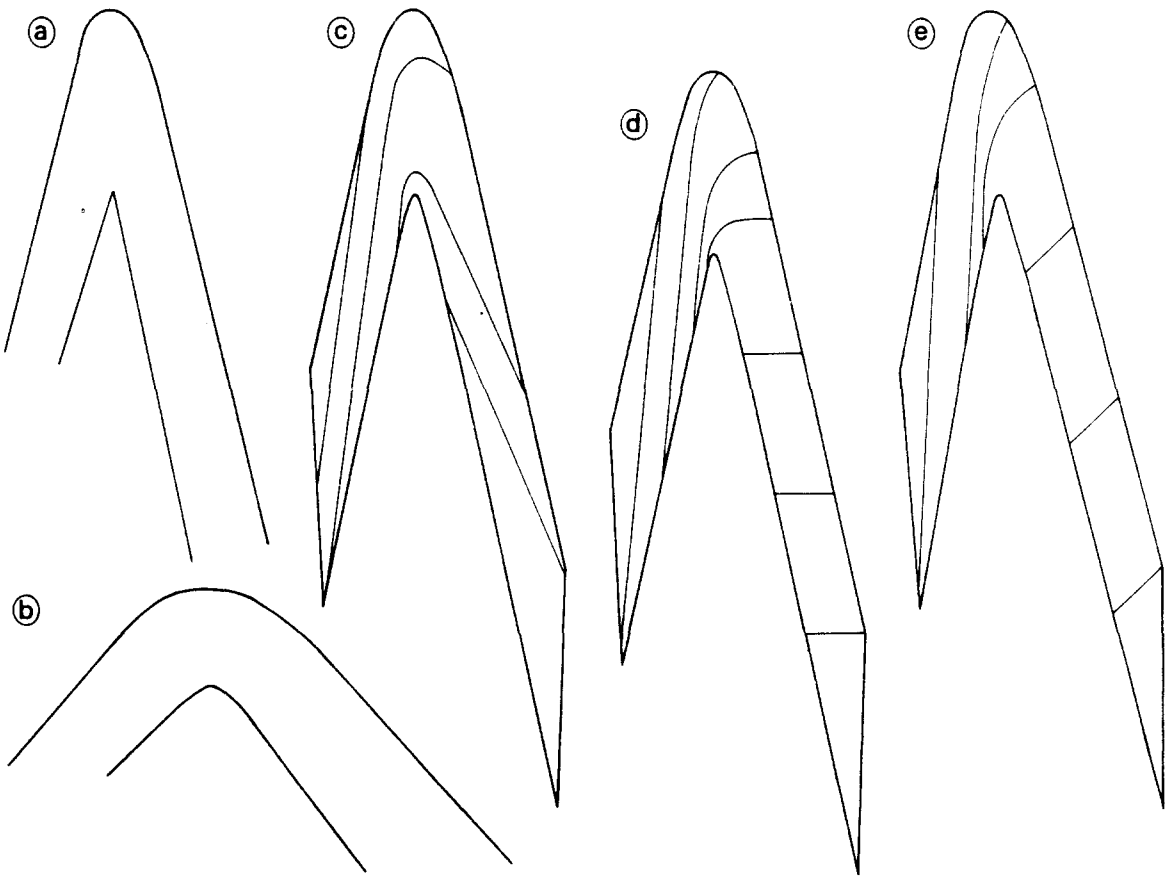

Fig. 6. Modification of cross-lamination by combination of flexural flow followed by homogeneous flattening. For further discussion see text. (a) Tracing of natural fold in siltstone. (b) Appearance of the same natural fold before flattening if it is assumed that fold developed by flexural flow followed by 48% homogeneous flattening. (c–e) Appearance of cross-lamination in hypothetical folds resembling (a) and developed by flexural flow followed by 48% homogeneous flattening. Assumed initial values of θ are (c) 15°, (d) 30° and (e) 35°. Figures constructed graphically.

possibility is difficult to assess, because if the strain is not orthogonal with the axial surface it will result in differences in bed thickness from one fold limb to the other. However, as noted above, variation in bed thickness is a primary feature of the beds considered here. In the orthogonal case, thickness variation was assumed to be primary in the fold limbs, and the amount of flattening was thus determined by averaging values obtained from different limbs. With two causes of thickness variation this is no longer possible. However, the possibility of oblique homogeneous flattening has been explored by trial and error for flattening values up to 50% with the principal axis of shortening inclined to the axial surface by 80° and by 70°, and with initial θ values of 15°, 30° and 35°. For these strain orientations, in contrast to the natural folds, the value of θ after straining is still smaller for right dipping limbs than for those dipping left.

Other orientations have not been considered because there is no reason to believe that the deformation path should include a late, homogeneous flattening that is not orthogonal with the axial surface, or that deformation is homogeneous in a heterogeneous body. Additionally the late conjugate cleavage indicates a shortening that is almost perpendicular to the axial surface of the folds.

A structure similar to that described here has been observed in folding experiments where the sequence of events involves initial folding with axial planes approximately perpendicular to the direction of shortening, followed by development of conjugate structures symmetric about the shortening direction and earlier fold axial surface (Williams & Means 1971). Thus the conjugate crenulation cleavage described here is interpreted as a product of late flattening, and hence it is suggested that the late shortening was inclined at about 80° to the earlier axial surfaces. Further, since it produced a heterogeneously distributed microfolding it is suggested that this strain was heterogeneous both on a fold and a micro scale.

TANGENTIAL LONGITUDINAL STRAIN FOLD MODEL

The flexural slip and shear fold models are defined in terms of fold mechanisms, and the mechanism prescribes the type of strain that can result from the folding. The tangential longitudinal strain fold model is different in that it is defined in terms of the resulting strain. It describes folds in which the strain axes are orthogonal with the folded surface (Ramsay 1967, p. 397). The strain is concentrated in the hinge, and a neutral surface separates areas of layer parallel extension from areas of layer parallel shortening. Thus strain models (a) and (c) (1967 fig. 9.20). Differences between the two stem strain fold model and there is good qualitative correspondence between the observed geometry of the folded cross-lamination and that predicted by Ramsay (1967 Fig. 9.20). Differences between the two stem from the fact that Ramsay has considered a fold in which the strain is symmetrical about the axial plane. In the natural folds considered here the strain is asymmetrical, but this can be explained by the asymmetry of the fold itself (see below).

OTHER FOLD MODELS

Strain models (b) and (d) (Fig. 4) are incompatible with the three simple fold models discussed above. They can both be considered as tangential longitudinal strain folds that are modified by a component of layer parallel shear in the fold limbs. In the case of (d) the sense of shear is the same as in a flexural slip fold, in (b) it is the opposite.

DISCUSSION

From the above discussion it follows that there are three possible fold models all of which can be defined in terms of the finite strain patterns that they produce. One is the tangential longitudinal flow strain model of Ramsay (ibid), and this corresponds to the strain models (a) and (c) presented in Fig. 4. The other two are the strain models (b) and (d) of Fig. 4. These four strain models are all equally possible descriptions of the strain in the natural folds, as noted above, but they are not all equally feasible in terms of kinematic models.

In all four models layer parallel components of strain in the hinge region are extensional on the convex side of the layer and compressional on the concave side. This can be expected to give rise to a layer parallel shear component of strain in the fold limb with the sense of shear as in a flexural slip fold. This is consistent with model (d) (Fig. 4) and is also observed in experimentally produced folds in such materials as rubber (Ramberg 1963), clay or wax (Ghosh 1966) and salt-mica 'schist' (Hobbs *et al.* 1976, fig. 4.35), and in numerical simulation of buckle folding (Dietrich 1969). Thus model (d) seems very reasonable. On the other hand it is difficult to imagine what could give rise to the reversed sense of shear of model (b). This model would require very special constraints and there is no reason to believe that such constraints exist; it is therefore the least attractive of the models. The same argument can be applied to a lesser extent to the tangential longitudinal flow models (a) and (c). These require a special pattern of strain in the fold hinge. If the limbs were completely unstrained it could be argued that its special nature was due to some work softening in the fold hinge, the limbs however, are also deformed. This model cannot be eliminated but it seems less reasonable than model (d).

The reason for the component of shear strain proposed for model (d) is that during folding, material on the concave side of the neutral surface is in compression, and material on the convex side is in extension. If volume is to be kept constant there will be an obvious tendency for strain in the fold limb to have a layer parallel shear component. However, if volume changes are possible, for example, by quartz migration as in the natural folds described here, or by the development of different mineral phases (Stephansson 1974), then the tendency for layer parallel shear will be reduced. Thus

layer parallel shear maybe less important in the folds described here than in, for example, experimentally deformed salt-mica aggregates (Hobbs *et al.* 1976, fig. 4.35), or in other natural folds where volume changes are more difficult.

DEFORMATION HISTORY

In view of the unusual amount of information that may be derived from relationships available in the specimen described here, an attempt is made to interpret its deformation history.

It has been suggested already that the finite strain in the competent layers most likely conformed to the pattern represented in Fig. 4(d). This interpretation is assumed to be correct for the purpose of the following model (Fig. 7).

On the scale of the bedding, it is suggested that straining began with a homogeneous layer parallel flattening. Such a flattening as a pre-folding stage has been postulated on the basis of theoretical work (Sherwin & Chapple 1968), and is observed in experiments (e.g. Ramberg 1964, Hobbs *et al.* 1976, p. 42). It is therefore suggested that there was such an initial shortening of unknown magnitude before initiation of the large folds. If this initial shortening produced foreset dips greater than those measured in either of the fold limbs then the layer parallel strain for the increment associated with the actual folding would have to be extensional in both limbs. During the initial shortening the axial plane

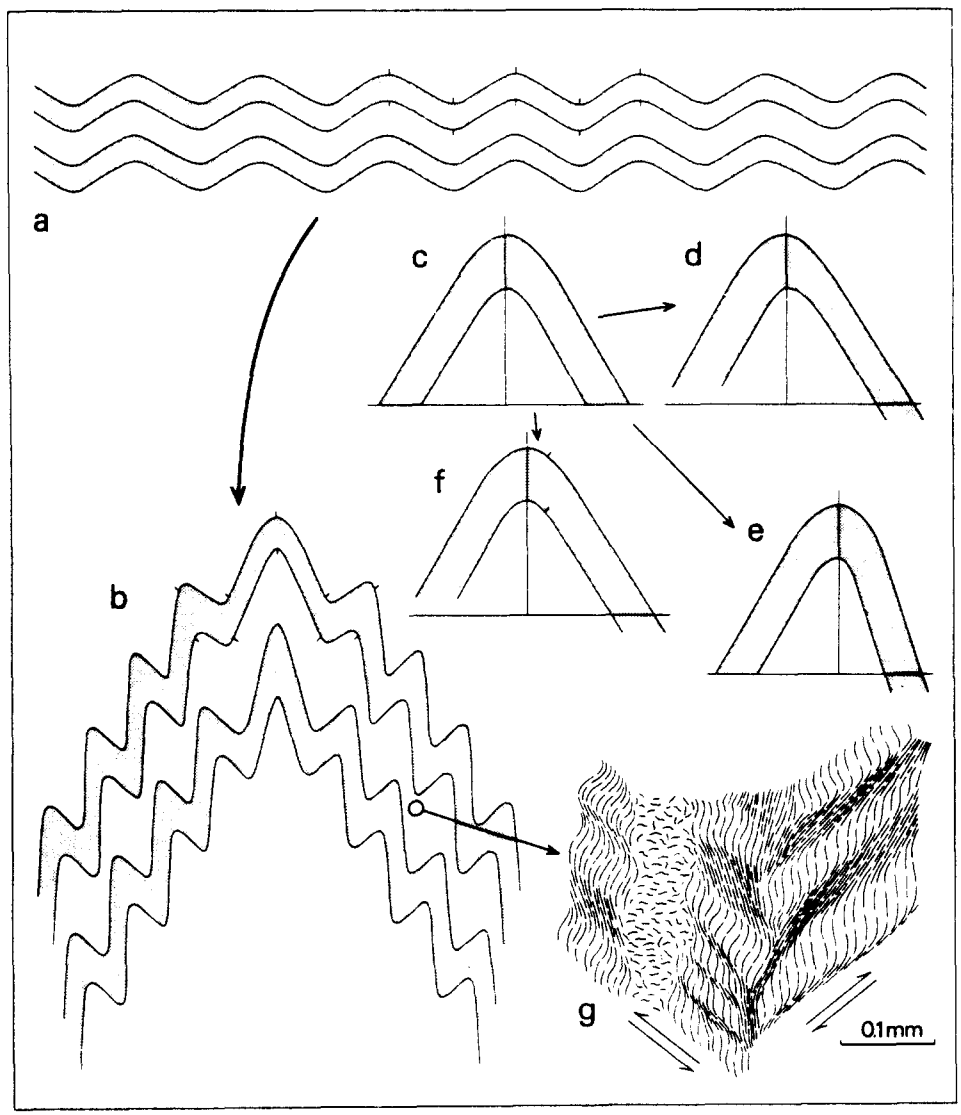

Fig. 7. Diagrammatic representation of deformation history. (a) Small symmetrical folds develop. (b) Larger structures develop and the small folds are constrained to become asymmetrical. Finally (g), conjugate crenulation cleavage develops symmetrically oriented with respect to the axial surface of the large folds. The N–S trending uncrenulated zone in (g) is a quartz-rich layer associated with the axial plane foliation. Diagrams (c–f) show ways in which symmetrical folds (c) can become asymmetrical. (d) by layer parallel shortening and extension of limbs, (e) by unequal rotation of limbs, and (f) by migration of fold hinges. All three methods are combined in (b) which is accurately constructed from (a). Ticks on bedding planes in (a), (b) and (f) indicate amount of dinge migration. See text for further discussion.

crenulation cleavage may have been initiated as symmetrical microfolds in the pelitic layers, and then at a later stage parasitic folds were initiated in the competent layers, before finally even larger folds were initiated (Fig. 7). Folding of the competent layers in the initial stages was achieved by virtually rigid body rotation of the limbs with some layer parallel shear strain, and by large internal strain in the fold hinge. This was accompanied by a strain with a large layer parallel component of shear in the incompetent pelitic layers. This could have been achieved by slip on an original bedding foliation if that were still planar, but because it was probably crenulated a more complicated mechanism seems likely. Thus it is suggested that this strain was achieved by an increase in the asymmetry of the crenulations which amounts to a heterogeneous simple shear component of strain parallel to the axial plane of the crenulations (and thus folds), plus a flattening perpendicular to their axial plane. This is consistent with the interpretation of the crenulation cleavage presented above, where the mica-rich domains become thinner by loss of quartz which may or may not be re-deposited in the microlithons in such a way as to make them longer (see Hobbs *et al.* 1976, fig. 5.23).

Thus it is suggested that, on the scale of the cleavage, differentiation started early in the deformation process. It is also suggested that on a larger scale once folds were initiated differences developed in the magnitude of mean stress from place to place in the fold and differentiation also began on that scale.

The large folds in the specimen are themselves parasitic to larger folds, and as deformation proceeded the smaller folds which were probably initially symmetrical, were constrained to become increasingly asymmetrical (Fig. 7). Three factors probably contributed to the development of this asymmetry. First, the dips of the fold limbs became asymmetrical. Second, layer parallel strain occurred in one or both limbs such that one limb appeared shortened relative to the other. Third, it is suggested that there was a localised migration of fold hinges.

Fold hinge migration is suggested not only because it is an obvious way of increasing the asymmetry of the parasitic folds, but also because it offers an explanation of the asymmetric form of the quartz-rich prisms (see Figs. 2 and 3). It is assumed that migration was accompanied by fold tightening, (see Fig. 8) and that during tightening the area of relatively low mean stress decreased in width. Thus one boundary, between areas from which quartz was being removed and areas from which it was not being removed and where it was perhaps even being deposited (i.e. the quartz-rich prism), must have migrated through the specimen. The other boundary, however, could have remained stationary or relatively so. Thus the latter can be expected to be sharper than the former, and the sharp boundary will be on the large antiform side of a parasitic antiform, and the large synform side of a parasitic synform.

The final deformation event appears to have been the development of a conjugate crenulation cleavage. A similar event has been observed in the development of experimental folds (Williams & Means 1971), and probably represents a locking of the folds. In the example described here the locking could be related to the increasing volume changes required to achieve successive increments of shortening perpendicular to the axial plane of the folds. In the experiments the conjugate cleavages are symmetrically related to the axial planes of the earlier folds, and the sense of movement is such as to continue the shortening perpendicular to the axial plane of the earlier folds. In the specimen described here the cleavages are asymmetric with respect to the folds, but these folds are parasitic on a larger fold, and the cleavages are symmetrically related to that fold. The sense of movement on the cleavages is the same as in the experimental folds.

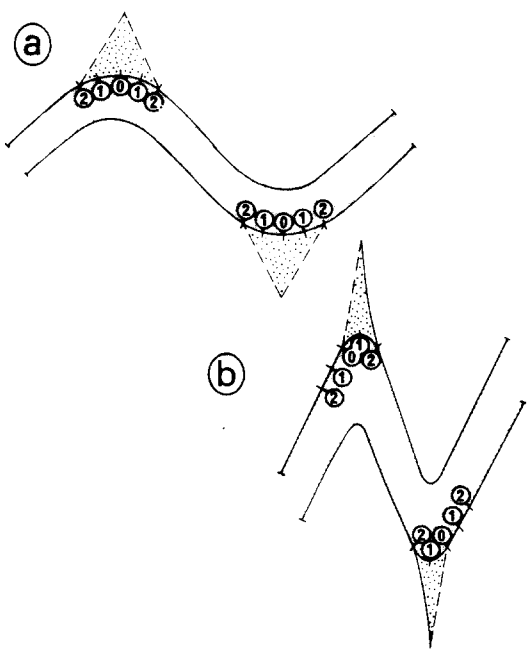

Fig. 8. Development of asymmetry of quartz-rich domains by migration of fold hinge. Ticks, numbered 0 to 2, are fixed reference points on the bedding surface. See text for further discussion.

APPLICABILITY TO OTHER FOLDS IN THE AREA

Lack of suitable continuously laminated beds elsewhere in the area makes it impossible to analyse

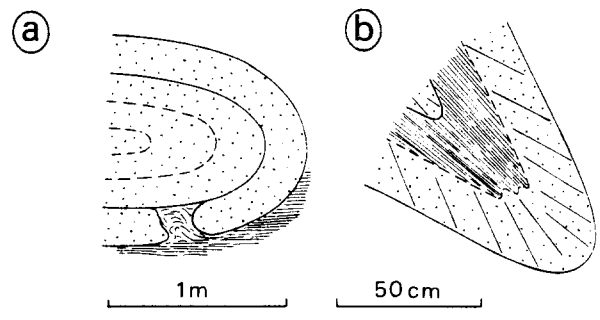

Fig. 9. Small folds showing features consistent with the strain pattern proposed here for development of folds in the competent layers. See text for discussion.

other folds in the same way. However, there is other evidence that suggests that the same mechanism may have operated. First, although it is not generally possible to follow a single cross bedded unit around a fold, cross bedded units are abundant and wherever they are exposed in fold limbs the foreset dips are close to 30°, even though the folds are as tight or tighter than the ones described here.

Although boudins are uncommon in the area some do occur in fold hinges but not in their limbs. They are present in the outer layer of sandstone packets where several closely spaced sandstone beds are separated by very thin pelitic layers (e.g. Fig. 9a).

Many of the folds described here are accompanied by disharmonic parasitic folds in the fold closures that occur on the concave sides of competent beds (e.g. Fig. 9b). The morphology of these folds resembles that of small folds which develop on the concave side of bent metal bars (see also Ramberg 1964, fig. 11), and they are consistent with the strain models proposed here.

Finally, a qualitative analysis of the orientation of sedimentary quartz grains indicates that they are commonly parallel to bedding in the competent layers in the fold limbs and on the convex side of the fold closure. On the concave side of such hinges, however, they are commonly rotated into the orientation of the axial plane foliation (e.g. Williams 1972, figs. 10 and 13). This orientation pattern is consistent with the finite strain picture presented here.

Acknowledgements—Fieldwork was supported by the University of Sydney, Australia, and drawings and photographs were prepared by staff of the Geology and Mineralogy Institute, Leiden.

The writer is grateful to B. E. Hobbs, G. S. Lister and R. J. Lisle for criticism of the manuscript at various stages in its preparation.

REFERENCES

Dieterich, J. H. 1969. Origin of cleavage in folded rocks. *Am. J. Sci.* **267**, 155–165.

Ghosh, S. K. 1966. Experimental test of buckling folds in relation to strain ellipsoid in simple shear deformations. *Tectonophysics* **3**, 169–185.

Hobbs, B. E. & Talbot, J. L. 1966. The analysis of strain in deformed rocks. *J. Geol.* **74**, 500–513.

Hobbs, B. E., Means, W. D. & Williams, P. F. 1976. *An Outline of Structural Geology*. John Wiley, New York.

Means, W. D. & Williams, P. F. 1972. Crenulation cleavage and faulting in an artificial salt-mica schist. *J. Geol.* **80**, 569–591.

Milnes, A. G. 1971. A model for analyzing the strain history of folded competent layers in deeper parts of orogenic belts. *Eclog. geol. Helv.* **64**, 335–342.

Pettijohn, F. J. 1957. Paleocurrents of Lake Superior Precambrian quartzites. *Bull. geol. Soc. Am.* **68**, 469–480.

Ramberg, H. 1963. Strain distribution and geometry of folds. *Bull. geol. Instn. Univ. Upsala* **B 42**, 1–20.

Ramberg, H. 1964. Selective buckling of composite layers with contrasted rheological properties, a theory for simultaneous formation of several orders of folds. *Tectonophysics* **1**, 307–341.

Ramsay, J. G. 1961. The effects of folding upon the orientation of sedimentation structures. *J. Geol.* **69**, 84–100.

Ramsay, J. G. 1967. *Folding and Fracturing of Rocks*. McGraw Hill, New York.

Ramsay, J. G. 1974. Development of chevron folds. *Bull. geol. Soc. Am.* **85**, 1741–1754.

Sherwin, J. A. & Chapple, W. M. 1968. Wavelengths of single layer folds: a comparison between theory and observation. *Am. J. Sci.* **266**, 167–179.

Stephansson, O. 1974. Stress induced diffusion during folding. *Tectonophysics* **22**, 233–251.

Williams, P. F. 1971. Structural analysis of Bermagui area, *J. geol. Soc. Aust.* **18**, 215–228.

Williams, P. F. 1972. Development of metamorphic layering and cleavage in low grade metamorphic rocks at Bermagui, Australia. *Am. J. Sci.* **272**, 1–47.

Williams, P. F. & Means, W. D. 1971. Folding experiments on an artificial schist. *Nature, Lond.* **234**, 90–92